Chapter 16 Assessment of Innovative Solutions for Non-Load Bearing Masonry Enclosures

João Leite¹, António A. Correia², Paulo B. Lourenço¹, Elizabeth Vintzileou³, Vassiliki Palieraki³, Paulo Candeias², Alfredo Campos Costa² and Ema Coelho²

¹ ISISE, University of Minho, Dept. of Civil Engineering, Guimarães, Portugal

² National Laboratory for Civil Engineering (LNEC), Dept. of Structures, Lisbon, Portugal

³ National Technical University of Athens (NTUA), Dept. of Structural Eng., Athens, Greece

Abstract In order to ensure that in-plane and out-of-plane damage of masonry infill walls due to seismic actions complies with the performance levels' requirements, Eurocode 8 imposes the use of reinforced solutions. Nevertheless, it does not provide any design rules or methodologies for such reinforced masonry enclosures. An experimental programme was thus defined for assessing the response of innovative solutions for non-load bearing masonry enclosures using LNEC's triaxial shake table. Two reinforcement solutions were tested on single leaf clay brick infill walls: (i) horizontal reinforcement in the bedding planes of the masonry units and (ii) reinforced mortar coating. Furthermore, a testing device for masonry infill panels was specifically conceived for this project. A detailed description of the methods used is given and the experimental results are partially presented and interpreted on the basis of the structural response and its evolution with damage.

16.1 Introduction

This paper presents some of the results of the research project "Masonry Enclosures" developed in the framework of the transnational access (TA) to LNEC's triaxial shake table within the FP7 project SERIES. The TA project addressed the seismic performance of masonry enclosures in European countries with moderate to high seismicity and how they affect the global structural response. It consisted on the experimental evaluation of the seismic response of reinforced concrete (RC) frames with innovative solutions for masonry infill walls, considering both the in-plane and out-of-plane behaviour of the enclosures.

The recent L'Aquila earthquake of 2009 has reminded seismic engineers that the current masonry infill solutions are not effective, as illustrated by the considerable in-plane damage and out-of-plane collapses verified in a common basis throughout the affected areas. Eurocode 8 (2010) addresses this issue by imposing the use of reinforced infill solutions but fails to give design and detailing methodologies. With the above in mind, a shake table experimental research programme was devised using two different approaches.

The first phase of the research activity involved the seismic testing of a twostorey RC frame building designed according to Eurocodes 2 and 8 (2010) and built at a 1:1.5 scale, schematically shown in Fig. 16.1 (a). As a follow-up of previous tests performed at LNEC, using RC buildings either with double leaf unreinforced masonry infill walls or with single leaf masonry plus bed joint reinforcement, this reduced scale model was built with single leaf clay bricks and a reinforced mortar coating: wire mesh reinforcement was placed within the mortar coating on both sides of the infill walls and anchored to the RC frame and masonry units. From these tests it was possible to assess the evolution of the seismic behaviour of infills and their influence on the RC structure through several acceleration inputs of increasing amplitude, associated to cumulative damage limit states.

The second phase of the TA project comprised four full-scale tests of closed RC plane frames infilled with masonry, simultaneously for in-plane and out-ofplane dynamic actions. Both unreinforced masonry infill walls and with horizontal reinforcement layers between masonry units were tested, with and without reinforcement in the mortar coating. The test setup simultaneously uses the shake table, one reaction wall and the Testing device for Innovative Masonry infills (TIM), as represented in Fig. 16.1 (b). This unique testing setup was specifically designed for these tests and is mainly composed of a stiff steel caisson threedimensional frame which moves rigidly with the shaking table. It is fixed to the specimen's upper beam in the transverse direction, while a system of rollers allows for an independent motion in the longitudinal direction. This phase of the TA project is presented herein conceptually, although no results are available yet.

The geometry of the reduced scale building model is shown in Fig. 16.1 (a). The dimensions of all models respect the typical dimensions for RC frames according to the survey in Pereira (2013). Moreover, traditional clay brick units, horizontally perforated, were used in all models.

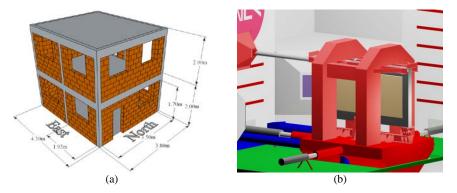


Fig. 16.1 Schematic representation of: (a) building model; (b) wall panels' test setup.

16.2 Building Model Tests

16.2.1 Building Specimen and Test Setup

The materials adopted for RC elements were C30/37 and S500 for concrete and steel reinforcing bars, respectively. All four façades of the model had infill walls: one façade without openings and around 20% of the area corresponding to openings in all other façades (see Fig. 16.2). The clay brick units used were only scaled in the thickness, while the other dimensions were kept at a 1:1 scale.

Cauchy-Froude similitude requirements between the prototype and the reduced scale model were duly respected during these tests (Carvalho, 1998). Namely, the specific mass of the model was modified by using two types of additional steel masses: 12 large masses in total (around 1.2 tonnes each) attached to the floor slabs and a set of 334 small masses (around 7 kg each) distributed throughout the walls of the building. The total weight of the mock-up (building model, RC foundation and additional masses) was nearly 434 kN.

The reinforced mortar coating adopted was composed of the reinforcement mesh Bekaert Armanet ϕ 1.05 mm 12.7 mm x 12.7 mm, a pre-batched M5 class mortar and the Hilti X-M8H10-37-P8 connectors for attaching the wire mesh to the RC elements, as illustrated in Fig. 16.3.

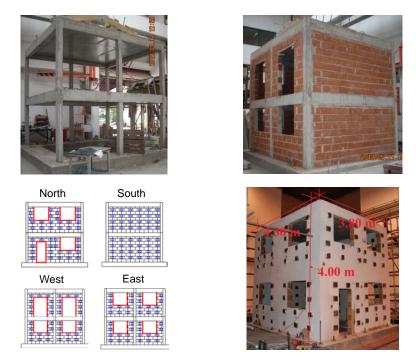


Fig. 16.2 Construction views and geometry of the reduced scale (1:1.5) building model.

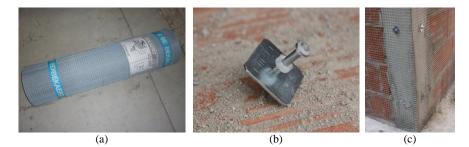


Fig. 16.3 Details of the wire mesh reinforcement application.

The abovementioned masses were used for connecting the wire mesh to the masonry units instead of the Hilti connectors, as shown in Fig. 16.2, since the former had to be used anyway in order to comply with the Cauchy-Froude similitude requirements.

After the RC foundation was attached to the shake table the model was thoroughly instrumented in order to characterize its behaviour during the tests. The instrumentation setup definition was based on the expected response of the model, obtained from preliminary studies (Leite, 2009), and the objectives of the test. The instrumentation can thus be divided in two groups: (i) setup to acquire the out-ofplane behaviour of the infill walls; (ii) setup to monitor the global response of the RC building. The out-of-plane behaviour of the infill walls was captured by a set of 34 accelerometers distributed on the surface of the walls according to Fig. 16.4. On the other hand, the global response of the RC frame was captured using a total of eight accelerometers placed orthogonally at the Northeast and Southwest corners of each RC slab.

Four motion detection cameras were also used at the corners of the slabs, as depicted in Fig. 16.5 (Hamamatsu, 2013). They are capable of determining the planar motion of an infrared LED each. The acquisition of all the equipment mentioned above was carried out using one SCXI chassis connected to a PXI-1001, both from National Instruments.

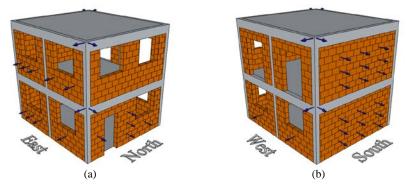


Fig. 16.4 Accelerometers setup for out-of-plane wall behaviour.

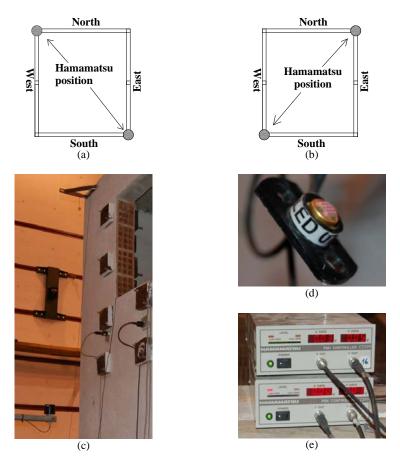


Fig. 16.5 Motion detection cameras: (a) position at first storey slab; (b) position at roof slab; (c) camera and led setup; (d) infrared led; (e) controller.

Additional measurements of out-of-plane motions at the North façade infill wall were carried out using the K600 camera system by Krypton (2003), composed of three CCD cameras that are able to track the 3D displacement of a set of infrared LEDs. The latter were spread on the upper floor wall, see Fig. 16.6.

16.2.2 Input Signal and Test Sequence

The seismic loading applied to the specimen was a bi-directional artificial horizontal ground motion, with uncorrelated components and around 30 s duration, fitted to the Eurocode 8 (2010) response spectra for Lisbon, Portugal, soil type A and seismic action type 1 (large magnitude, long distance). It was applied in three stages of increasing amplitude associated to cumulative damage limit states.

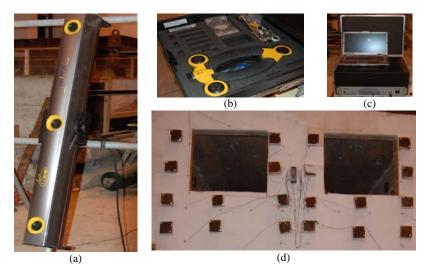


Fig. 16.6 K600 camera system by Krypton (2003): (a) CCD cameras; (b) calibration equipment; (c) acquisition system; (d) LEDs distributed on the upper floor infill wall of the North façade.

Six artificial accelerograms were generated (Mendes, 2008), resulting in a pair of accelerograms for each stage of the shake table tests. The accelerograms were fitted to the 5% damped elastic response spectra of Eurocode 8 (2010), scaled according to the damage state considered for each stage: Damage Limitation (DL - 225 years of return period (YRP)); Significant Damage (SD - 475 YRP); Near Collapse (NC - 2475 YRP). Fig. 16.7 represents the longitudinal component of such ground motions, which comply with the Cauchy-Froude similitude requirements, thus evidencing a time contraction with respect to the code spectral values, by a factor of $1.5^{1/2}$, but no scaling in the acceleration values. The test sequence consisted on the application of these three stages, while performing dynamic identification tests in between them, as shown in Table 16.1.

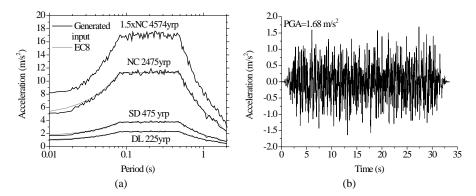


Fig. 16.7 Longitudinal (North-South) component of horizontal ground motion: (a) pseudo-acceleration response spectra; (b) target accelerogram for stage 2 (SD).

Stage	Identification	Description
1	DI 0	Initial dynamic identification test
	DL	Seismic test for Damage Limitation limit state
	DI 1	Dynamic identification at the end of stage 1
2	SD	Seismic test for Significant Damage limit state
	DI 2	Dynamic identification at the end of stage 2
3	NC	Seismic test for Near Collapse limit state
	DI 3	Dynamic identification at the end of stage 3

Table 16.1 Shake table test sequence for the building specimen

16.2.3 Results and Discussion

16.2.3.1 Overall response and damage evolution

The specimen did not show any visual signs of damage after stage 1. However, during stage 2, cracks developed in the mortar coating at all four corners of the building, starting at its base, and between the window jambs on the intermediate columns of the East and West façades. Small cracks starting at the corners of some of the ground floor openings and moving towards the RC frame were also visible, whilst the first floor presented almost no damage. Fig. 16.8 presents the crack patterns after stage 2 (and 3). These results are in agreement with the dynamic data, which shows a frequency decrease of 3.1% on average for all relevant modes and with respect to the initial state. Such stiffness loss can be related to the separation of the infill walls from the RC frame and to micro-cracking in the RC structure. This damage is either difficult to detect or camouflaged by the mortar coating.

After the third stage, the building presented wider and longer cracks and some mortar coating detachment at all corners of the ground floor, as shown in Fig. 16.9 (b) and (d). Considerable cracking was present between the window jambs at the ground level of the East and West façades, see Fig. 16.9 (c), as well as at the corners of the North façade openings, see Fig. 16.9 (a). Globally, the structure presented light damage, given the amplitude of the first three stages of the test, and concentrated at the ground level. However, analysis of the dynamic data showed a frequency decrease of 22.1% on average for all relevant modes and with respect to the initial state, suggesting a more extensive damage than the apparent one.

It is pointed out that during the application of the seismic input of stage 3 there were some difficulties on the shake table control, leading to a larger than desired input motion for frequencies above 4 Hz. For this reason, and given the light overall damage in the specimen, it was submitted to the first three stages again. As shown in Fig. 16.10, this attempt also failed to fulfil the stage 3 target motion.

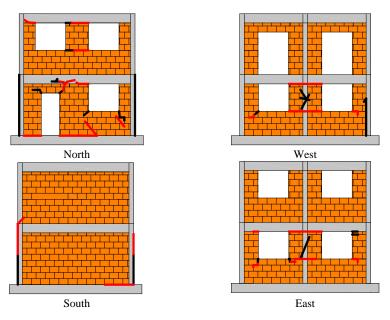


Fig. 16.8 Crack patterns after stages 2 (black lines) and 3 (red lines) – Note: the lines on the RC frame represent damage on the mortar coating, not necessarily on the RC frame.

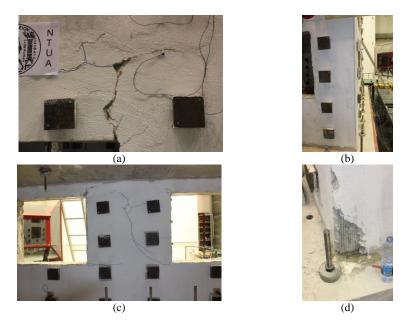


Fig. 16.9 Damage after stage 3: (a) extensive cracking at the corner of the ground floor window of the North façade; (b) cracking in the coating along the height of the Northwest corner; (c) cracks at the West façade window jambs of the ground floor; (d) coating detachment at the base of the Southwest corner.

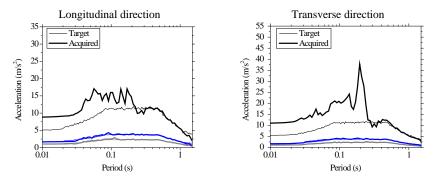


Fig. 16.10 Target and measured pseudo-acceleration response spectra for the additional tests.

After the additional three test stages, the specimen did not develop new cracking patterns but the existing ones widened considerably, see Fig. 16.11. On the other hand, the mortar coating became increasingly detached from the infill walls, apparently depending completely on the connection provided by the additional masses. These results highlight the importance of establishing a good connection of the reinforced coating to the infill walls. Regarding the upper storey, it presented no significant damage, with nothing but small cracks forming at the corners of the openings.

Upon removal of the additional masses, it was apparent that the reinforced coating was completely detached from the infill walls and that the supports of the additional masses worked as connectors, thus preventing the mortar coating from collapsing. Moreover, a careful analysis of the infill walls showed that, although these presented limited damage, they were overall disconnected from the RC frame. This implies that there was a major contribution of the reinforced coating in preventing the out-of-plane collapse of the infill walls. Regarding the RC structure, extensive cracking was detected at some of the beam-column connections, as shown in Fig. 16.12. The RC frame was very flexible under these conditions, meaning that the reinforced coating may have contributed significantly to prevent the collapse of the entire specimen.

16.2.3.2 Evolution of modal properties

The evolution of the five lower vibration frequencies of the building model, detected during the dynamic identification tests (DI 0 to DI 3), are herein used for illustrating the structural degradation of the specimen. The initial modes of vibration (DI 0), with frequencies ranging from 6.3 Hz to 35.6 Hz, are plotted in Fig. 16.13: the first two longitudinal and transverse modes and the first torsional one.

Fig. 16.14 (a) presents the evolution of the frequencies with the test stages for each of the five modes. Additionally, Fig. 16.14 (b) presents a similar evolution for out-of-plane vibration modes of the infill walls.



Fig. 16.11 Damage after additional seismic tests: (a) North façade; (b) crack and mortar rendering loss at the Northwest corner; (c) crack at the interior jambs in the infill wall at the ground floor of the East façade; (d) South façade; (e) crack at the a lateral jamb in the infill wall at the ground floor of the East façade; (f) crack and mortar rendering loss at Northeast corner.



Fig. 16.12 Extensive cracking observed upon reinforced coating removal at the beam-column connection in the Northwest corner.

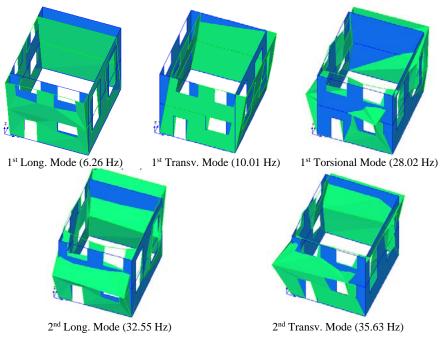


Fig. 16.13 Initial vibration modes and frequencies of the building model on the shake table.

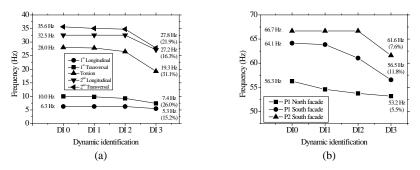


Fig. 16.14 Evolution of the vibration frequencies along the test stages and final reduction with respect to the initial state: (a) initial five global vibration modes of the building; (b) out-of-plane vibration modes of the infill walls.

After stage 2, the longitudinal direction presented no frequency decrease, the transverse direction presented an average 5.1% decrease and the torsional mode presented a 5.5% decrease, in comparison to DI 0. After stage 3, the average decrease in the longitudinal direction was 15.8% and the average frequency loss in the transverse direction was 24.0%. This larger stiffness loss in the transverse direction is related to the larger dependence of the transverse vibration modes on the behaviour of the infill walls. As these get detached from the RC frame, due to in-

plane damage, the overall stiffness decreases and so does the frequency. The infill walls contributing to the stiffness in the longitudinal direction also detach from the RC frame; however, the response in this direction is more dependent on the RC frame and less dependent on the infill walls. Finally, the torsional mode presented a 31.1% frequency decrease, possibly associated to a loss of connection between the infill walls and the RC frame since the high frequency of the torsional mode is very dependent on the response of the infill walls (Leite, 2009). This evolution of dynamic properties is in agreement with the observed overall damage.

Fig. 16.15 depicts seismic vulnerability curves, for each vibration mode of the building specimen, in terms of relative frequency decrease versus the seismic input energy as intensity measure. These confirm that the longitudinal direction presented no considerable damage until stage 3. After this stage, the transverse direction presented considerably more damage when compared to the longitudinal one, which is clearly associated to a larger energy input.

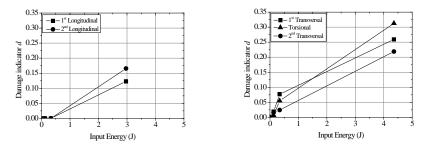


Fig. 16.15 Seismic vulnerability curves using the input energy as intensity measure.

16.2.3.3 Displacement demand

The maximum values of the floor displacements and interstorey drifts measured in the building model during the three test stages increase progressively with the seismic amplitude, as shown in Fig. 16.16. The first floor displacements and its drift with respect to the ground floor reached similar values in both directions for all three stages, while the roof displacements were slightly larger in the longitudinal direction, according to the first mode shape, even though the second mode presented a larger frequency decrease. These results are in agreement with the observed damage and modal frequencies variation, since both directions show similar responses in the first two stages, which did not damage the model, while in the third stage both directions register large displacement and drift increments.

The maximum values of the interstorey drift were, in general, larger on the upper floor than on the lower floor. Nevertheless, their difference decreased as the seismic intensity increased. The exception to the former trends occurred for stage 3 in the transverse direction: the interstorey drift at the upper floor was much smaller than the one at the lower floor and the one in the longitudinal direction.

Similar comments can be made on the basis of the results obtained in the additional seismic tests, presented in Fig. 16.17. Nevertheless, the maximum values of the floor displacements and interstorey drifts were significantly larger than the ones obtained on the first set of three test stages.

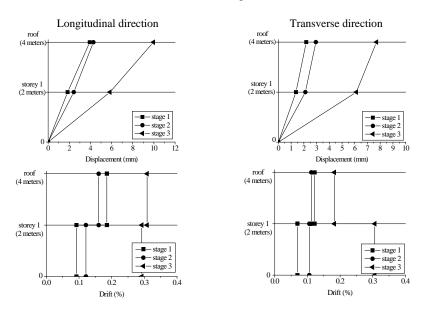


Fig. 16.16 Maximum interstorey displacements and drifts.

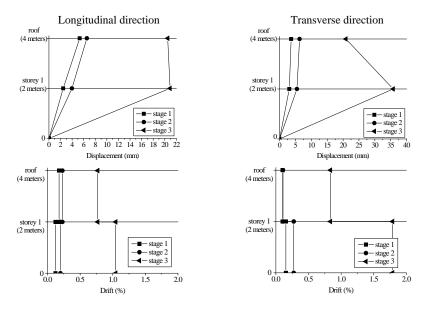


Fig. 16.17 Maximum interstorey displacements and drifts for the additional tests.

16.2.3.4 Comparison with previous tests

Two building models, similar to the specimen analysed within this project, were previously tested at the Earthquake Engineering and Structural Dynamics Division (NESDE) of LNEC. The first one, model 1, was designed following the Portuguese pre-Eurocode normative, RSA and REBAP (1983), and built with the most commonly used classes for concrete and steel reinforcing bars (C20/25 and S400, respectively). The masonry infill walls were built with double leaf, unreinforced, clay brick units. Hence, model 1 represents the built heritage in Portugal for the last three decades. The second specimen, model 2, was designed according to Eurocodes 2 and 8 (2010) and built with concrete and steel reinforcing bars of higher classes (C30/37 and S500, respectively), together with single leaf clay brick infill walls with bed joint reinforcement. The latter was connected to the RC frame with steel dowels at every second bed joint. The reason to use a single leaf is to place an external thermal insulation system. Therefore, model 2 and the specimen built within this project (model 3) represent possible solutions to be adopted in the construction of future RC frames with masonry infills.

All models were subjected to the same three seismic input stages described previously. Additionally, models 1 and 2 were subjected to a fourth stage with an input motion corresponding to 1.5 times the one from stage 3 (return period of 4574 years), as shown in Fig. 16.7.

Model 1 had a good performance until the end of stage 2, with no visible damage. Nevertheless, both the RC frame and the infill walls clearly showed a frequency loss. During stage 3, some of the thin masonry units, applied on the external leaf outside the RC columns and beams in order to avoid thermal bridges (a very common solution in the Portuguese building stock), cracked and fell. During stage 4 the double leaf unreinforced infill walls of the ground floor performed poorly, collapsing out-of-plane by a rigid-body rotation around the base of the model. In the following, a highly undesirable *soft-storey* collapse mechanism developed, with a low energy dissipation capacity and a brittle behaviour. Both the interior and exterior leaves presented a similar seismic behaviour.

Regarding model 2, the single leaf infill walls with bed joint reinforcement connected to the RC frame also presented a very good seismic performance until the end of stage 2, with no visible damage and only a small decrease in the modal frequencies of the structure. After stage 3, the unreinforced mortar coating was severely damaged, especially at the corners of the model. The model did not collapse during stage 4 but presented severe, and most likely irreparable, damage. Moreover, despite Eurocode 8 (2010) imposes a structural detailing in order to ensure a *beam-sway* mechanism, the RC structure developed a *soft-storey* mechanism. Taking into account the mid-height cracks that developed at all RC columns, it is possible to assume that the infill walls and their openings influenced negatively the seismic response of the RC structure. None of the infill walls collapsed out-of-plane, but it was clear that the ones with openings at the ground floor would collapse if there was no bed joint reinforcement and a connection to the RC frame.

16.3 Wall Panels Tests

16.3.1 Wall Panels Specimens and Test Setup

The second part of this transnational access activity comprised the dynamic testing of a closed RC plane frame with external dimensions of 6.40 m x 3.25 m. The structural elements of this frame had cross-sectional dimensions of 0.5 m x 0.4 m (beams) and 0.4 m x 0.4 m (columns). These specimens were tested simultaneously for in-plane and out-of-plane dynamic actions, representing the response of a 4th floor frame panel of an 8-storey RC building (see Fig. 16.18). The columns have 360 kN of centred prestress, representing the vertical load from the floors above.

The first two masonry enclosure solutions tested were the unreinforced masonry and the one with horizontal reinforcement between masonry units (Bekaert Murfor RND/Z-5-200). Afterwards, both masonry infills were demolished and rebuilt, inside the same RC frames, using a reinforced mortar coating. Fig. 16.19 illustrates the construction process of the models.

As mentioned in the introduction, the test setup for the wall panels simultaneously uses the shake table, one reaction wall and the Testing device for Innovative Masonry infills (TIM), as represented in Fig. 16.1 (b).

The in-plane motion enforces an inter-storey drift time-history on the frame by restraining the upper beam and by imposing the displacement of the shake table on the lower beam. The upper beam, which also has 360 kN of centred prestress for withstanding push-pull actions, is prevented from moving in the longitudinal direction through a strut connection to the reaction wall. This connection between the strut and the reaction wall is performed via a pyramidal support, as depicted in Fig. 16.20 (a), which distributes the strut reaction on the wall. A long rod then links the pyramidal support to the RC frame upper beam through hinged connectors. All beam-column joints are free to rotate in the plane of the infill, through special hinged base supports, visible in Fig. 16.20 (a).

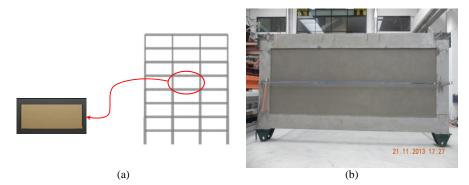


Fig. 16.18 Wall panel of typical RC frame building: (a) schematic view; (b) test specimen.



Fig. 16.19 Masonry infill construction with bed joint reinforcement.

On the other hand, the out-of-plane motion consists on a rigid-body vibration of both the upper and lower beams, reproducing the storey absolute accelerations and thus inducing high-frequency inertia forces perpendicular to the masonry panel and leading to a local vibration of the infill wall. Note that this shake table motion is transmitted to the top beam through the rigid steel caisson structure of TIM. The design of TIM was thus controlled by the requirement of a very stiff behaviour in the transverse direction, which was ensured by a vibration frequency for the first mode of vibration above 20 Hz. The entire test setup is shown in Fig. 16.20 (b).



Fig. 16.20 Wall panels test setup: (a) Hinged base and pyramidal support; (b) complete setup.

The instrumentation of the wall panels comprised several different sensors:

- (i) K600 camera system by Krypton (2003) for measuring the out-ofplane deformations of the wall panel using 16 leds (Fig. 16.21);
- (ii) Video camera for measuring the RC node in-plane deformation using data image correlation methods (Fig. 16.22);
- (iii) Optical system by Hamamatsu (2013) for measuring horizontal motions of the bottom and top corners of the RC frame (Fig. 16.23);
- (iv) 36 accelerometers for vibration monitoring of the shake table, TIM, RC frame and masonry wall panel (Fig. 16.23);
- (v) Load cells for measuring the dynamic reaction on the strut connecting the reaction wall and the top beam of the RC frame (Fig. 16.24).



Fig. 16.21 Out-of-plane wall panel deformation measurement system (Krypton, 2003).



Fig. 16.22 Video camera and target points for data image correlation measurement of in-plane deformations at one RC frame node.

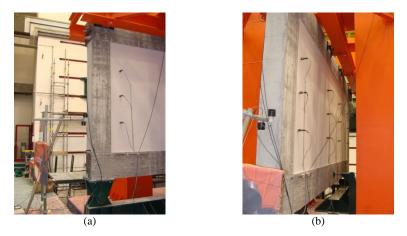


Fig. 16.23 (a) Hamamatsu (2013) setup for measuring horizontal translations of the RC frame nodes; (b) accelerometer setup for out-of-plane vibration measurements.

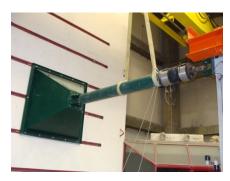


Fig. 16.24 Load cells for strut reaction measurement.

16.3.2 Input Signal and Test Sequence

The same seismic inputs used for the building specimen were adopted in the wall panels' tests, except that the latter are at full scale. These accelerograms were applied at the base of a representative building model, represented in Fig. 16.25, in order to obtain the time-history of the wall panels' motions.

The response time-history in terms of interstorey drift at the 4th floor for the seismic input considered corresponds to the shake table motion to be applied in the longitudinal direction. On the other hand, the absolute acceleration observed in the out-of-plane direction corresponds to the shake table motion transmitted by TIM to the masonry panel inside the RC frame. Both longitudinal and transverse motions are represented in Fig. 16.25.

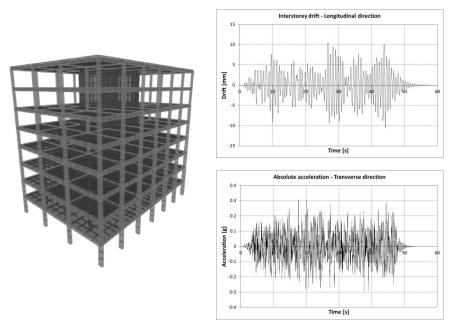


Fig. 16.25 Representative building model for wall panel input time-histories definition and resulting in-plane (longitudinal) and out-of-plane (transverse) time-histories.

16.4 Conclusions

Reinforced masonry infill wall solutions able to comply with the performance levels' requirements of Eurocode 8 (2010) were tested using LNEC's triaxial shake table. The building model, thoroughly described in this work, used single leaf clay brick infill walls with a reinforced mortar coating. This solution presented only minor damage for a seismic input corresponding to the Significant Damage limit state (475 years of return period) and light damage for a seismic input corresponding to the Near Collapse limit state (2475 years of return period).

After additional tests were performed, with a repetition of the three test stages, the building still presented light damage for a visual observation. Nevertheless, there was a considerable stiffness loss of the specimen. After the removal of the reinforced coating, it was possible to verify that the RC columns did not present plastic hinges at the extremities neither cracks at mid-height, despite considerable cracking at some beam-column joints, hence no undesirable collapse mechanism developed. It may be concluded that the infill walls had no negative influence on the seismic performance of the RC structure, unlike what happened in a previous test using bed joint reinforcement.

The infill walls were not significantly damaged after all test stages, even though the dynamic identification presented a clear stiffness loss. This was due to the observed detachment between the reinforced coating and the infill walls and between these and the RC frame, which allowed for relative motions of the RC frame with respect to the infill walls. Finally, although the reinforced coating concealed the damage on the infill walls, it prevented their out-of-plane collapse.

The second phase of the project included the development of an innovative testing setup and methodology for conducting full-scale seismic tests on wall panels. These were presented only conceptually, but preliminary results seem promising.

References

- Carvalho EC (1998) Seismic testing of structures. Proc. of the 11th European Conference on Earthquake Engineering, Paris, France
- Eurocode 2 (2010) NP EN 1992-1-1. Eurocódigo 2 Projecto de estruturas de betão Parte 1-1: Regras gerais e regras para edifícios. Portuguese Institute for Quality (IPQ), Lisbon, Portugal
- Eurocode 8 (2010) NP EN 1998-1. Eurocódigo 8 Projecto de estruturas para resistência aos sismos - Parte 1: Regras gerais, acções sísmicas e regras para edifícios. Portuguese Institute for Quality (IPQ), Lisbon, Portugal
- Hamamatsu (2013) C5949 characteristics. At http://pdf.datasheetcatalog.com/datasheet/hamamatsu/C5949.pdf (accessed on 30/6/2013)
- Krypton (2003) K400/K600 Hardware & Software Guide (Krypton Help Pages), Leuven, Belgium
- Leite J (2009) Avaliação da segurança baseada em deslocamentos: aplicação a edifícios de betão armado sem e com paredes de preenchimento (in Portuguese). MSc Dissertation, Dept. of Civil Engineering, University of Minho, Guimarães, Portugal
- Mendes L (2008) LNEC-SPA: Signal Processing and Analysis Tools for Civil Engineers. Earthquake Engineering and Structural Dynamics Division, Dept. of Structures, National Laboratory for Civil Engineering (LNEC), Lisbon, Portugal
- Pereira MFP (2013) Avaliação do desempenho das envolventes dos edifícios face à acção dos sismos (in Portuguese). PhD Thesis, Dept. of Civil Engineering, University of Minho, Guimarães, Portugal
- REBAP (1983) Regulamento de Estruturas de Betão Armado e Pré-Esforçado. Diário da República, Portugal
- RSA (1983) Regulamento de Segurança e Acções para Estruturas de Edifícios e Pontes. Diário da República, Portugal